Aust. J. Phys., 1990, **43**, 765–78

An Experimental Investigation of Electron Transport in $E \times B$ Discharges

M. J. Brennan[A] *and A. M. Garvie*[B]

Institute for Atomic Studies,
Flinders University of South Australia,
Bedford Park, S.A. 5042, Australia.
[A] Present address: Atomic and Molecular Physics Laboratories,
Research School of Physical Sciences, Australian National University,
G.P.O. Box 4, Canberra, A.C.T. 2601, Australia.
[B] Present address: Weber Research Institute,
Polytechnic University, Route 110,
Farmingdale, NY 11735, U.S.A.

Abstract

The 'photon flux' technique has been used to study electron transport in molecular nitrogen for steady stream discharges under the influence of $\boldsymbol{E} \times \boldsymbol{B}$ fields. The results, the first for the range of conditions $350 < E/N < 550$ Td, $0 < B/N < 1009 \times 10^{-17}$ G cm^3, are reported and comparisons between the experimentally determined transport parameters and those obtained under similar conditions by Monte Carlo simulation are made.

1. Introduction

At low values of the reduced electric field, E/N, the results of experiments in non self-sustained discharges may be compared with those gained from solutions of the Boltzmann equation, or Monte Carlo simulations, to verify the accuracy of the collision cross-section data used in the computations (Crompton 1983). This is only possible because of the relatively small number of collision processes that may occur. However, the unique determination of collision cross sections in discharges with higher mean energies has stimulated attempts to measure more parameters characterising discharge behaviour, such as excitation rates (see e.g. Jelenkovic and Phelps 1987; Phelps and Pitchford 1985; Tachibana and Phelps 1979).

Collision cross sections in an accurate gas model must predict the transport parameters for discharge conditions where hydrodynamic transport theory provides an accurate description of the discharge development. The superposition of a magnetic field, perpendicular to the electric field, changes the discharge conditions and the energy dependence of the distribution function. The transport data measured for this configuration provide additional information for comparison with simulated values and thus this configuration can provide a useful cross check on cross-section data derived by other means.

By observing the spatial and/or temporal variation of the photon flux from decaying molecules, previously excited by electron impact, the transport parameters for electron swarms in non self-sustaining discharges may be

0004-9506/90/060765$03.00

deduced. The experimental method, known as the 'photon flux' technique, is well established for electron swarms under the influence of an accelerating electric field (see e.g. Blevin 1985; Wedding *et al.* 1985). Recently, Brennan *et al.* (1990) have discussed the application of the method to the $\boldsymbol{E}\times\boldsymbol{B}$ geometry.

This paper describes measurements of electron transport parameters in steady-state non self-sustaining discharges in $\boldsymbol{E}\times\boldsymbol{B}$ fields in nitrogen. The measurements, under conditions where the electron cyclotron frequency is of the order of the electron–molecule collision frequency, are compared with the results of Monte Carlo simulations under similar conditions, using a model for nitrogen proposed by Ohmori *et al.* (1988). It follows the model of Tagashira *et al.* (1980), incorporating changes which were necessary to achieve better agreement with the transport data of Wedding *et al.*, derived from photon flux experiments in an accelerating electric field.

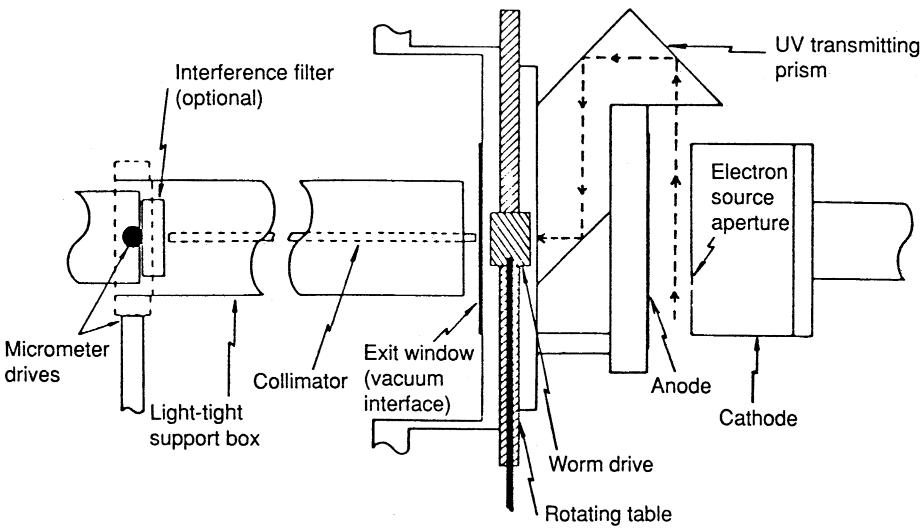

Fig. 1. Schematic diagram of the apparatus, detailing the relationship between the UV prism, the rotating table, the drift region between anode and cathode and the photo-detection optics. The dashed line traces the optical path of a ray, originating from the body of the discharge, through the prism to the exit window.

2. Experimental Apparatus

A schematic diagram of the apparatus used in these investigations is shown in Fig. 1 which details the arrangement of the drift region, the electron source and a rotating table and prism arrangement, used for detecting the photon flux. A plane–plane electrode system was used. The cathode was 5 cm in diameter with a 1·1 mm aperture, through which electrons were admitted to the drift region. This was off-set from the axial centre of the cathode by 1 cm to allow the electrons to drift towards the symmetry axis of the electrodes under the influence of the applied magnetic field. This helped ensure that field non-uniformities, due to the finite diameter of the electrodes, had a negligible effect on the measured transport parameters when magnetic fields were applied.

The electron source, an indirectly heated oxide coated cathode, was mounted behind the negative electrode, which acted as a 'light tight' shield against photons emitted by the electron source. The electrons were injected in a steady stream into the drift region by a small potential difference (typically ~8 V) between the filament and the cathode. The discharge current (typically 75 nA) provided feedback to the filament power supply through an optical isolator. This allowed the discharge current to be held constant to within $0\cdot5\%$ for the duration of the experiment [~4 hours per (E/N, B/N) combination].

The anode, $5\cdot5$ cm in diameter, was located in a bed of machinable ceramic (see Fig. 1), which ensured that all the current collected passed to earth through a Keithly model 480 picoammeter, used to sense the discharge current for the filament power supply feedback circuit. Experiments were conducted with a typical inter-electrode spacing of $1\cdot25$ cm at pressures of the order 1 Torr (≡133 Pa). The purity of the filling gas, nitrogen, was quoted as $99\cdot9995\%$ by the supplier, the British Oxygen Company Ltd. However, outgassing of parts of the apparatus, particularly those heated by the electron source, led to typical impurity levels of 1 part/1000. Although no 'guard-rings' were used between the electrodes, the close agreement between the present results at zero magnetic field strength and those of Wedding *et al.* (1985) suggests that any non-uniformities in the electric field had a negligible effect on the results of this study.

A pair of electromagnets, mounted orthogonally with respect to the two electrodes, produced a magnetic field of up to 350 G. The electromagnets were spaced such that the resulting magnetic field was uniform to within 2% in the region between the electrodes. Spatial variations in the magnetic field were mapped by a Hall probe, which was then used as a monitor, external to the apparatus, to guard against long term temporal variation in the constant current power supply for the electromagnets.

A theoretical treatment of swarm development in $\boldsymbol{E}\times\boldsymbol{B}$ fields, detailed in Blevin and Brennan (1983) and Brennan *et al.* (1990), relates the production of excited states in steady-state non self-sustained discharges, integrated along 'lines of sight', to the electron number density. According to this treatment, the discharge is characterised at several points along the symmetry axis of the electrodes (this is effectively a difference measurement) by experimentally probing the variations in the photon flux from many lines of sight, which are orthogonal to the electrode symmetry axis (see Section 3). To measure the photon flux from the two angles required by the theory described in Section 3, a prism attached to a rotating table, which could be driven to positions about the electrode symmetry axis by a worm drive connected to a rotating vacuum feed-through, was used to direct the photon flux emitted from the discharge through one of the end flanges in the apparatus. The prism and exit window were made from a fused silica, Herasil 1, to allow optimum transmission of discharge emissions in the UV. These include the $C^3\Pi_u$–$B^3\Pi_g(0\text{–}0)$ transition at $337\cdot1$ nm, which dominates emission spectra for the conditions studied, and the $B^2\Sigma_u^+$–$X^2\Sigma_u^+(0\text{–}0)$ at $391\cdot4$ nm, another important transition studied in this work. The discharge was 'viewed' through the exit window by a collimator which had a resolution of $0\cdot95$ mm FWHM at the centre of the electrodes. The collimated photon flux was detected using Centronics type Q4182 or P4249 low noise photomultipliers. The resulting signals were amplified and the unipolar output of a double delay line amplifier was counted by a scalar, gated for a pre-set time. The collimator and photomultiplier assembly could be positioned to view any position on the exit window using a micrometer X–Y movement in a 'light tight' box. This arrangement could re-position the collimator to an accuracy of better than $0 \cdot 1$ mm. The discharge currents used and the geometry of the detection system, ensured that counting errors due to 'pulse pile-up' could be ignored. In addition, the relatively low current densities normally used ensured that the presence of space charge and energetic nitrogen meta-stable molecules had no detectable effect on the discharges studied. The prism and rotating table arrangement in fact made it possible to view the drift region from any angle without restrictions to access imposed by the field coils. As illustrated in Fig. 1, an interference filter could be placed between the photomultiplier and the collimator, allowing the spatial distribution of photons corresponding to individual transitions to be monitored. In a companion paper [Garvie and Brennan (1990); present issue p. 779, hereafter referred to as GB], observations of the photon flux from different excited states are made at many angles, using the rotating prism and an appropriate interference filter. This allows a tomographic study of the emission from discrete excited states in an $\boldsymbol{E}\times\boldsymbol{B}$ discharge to be made.

3. Data Analysis

The 'equilibrium' region of a non self-sustained Townsend discharge in an $\boldsymbol{E}\times\boldsymbol{B}$ field may be defined as the region where the 'velocity symmetric' part of the electron energy distribution function, $f_0(\boldsymbol{r},\epsilon,t)$, can be represented in general by a first order expansion in the spatial density gradient:

$$f_0(\boldsymbol{r},\epsilon,t) = n(\boldsymbol{r},t)\, g^{000}(\epsilon) - \frac{1}{N} g^{100}(\epsilon)\frac{\partial n}{\partial X} - \frac{1}{N} g^{001}(\epsilon)\frac{\partial n}{\partial Z}, \tag{1}$$

where

$$\int_0^\infty g^{000}(\epsilon)\, d\epsilon = 1, \qquad \int_0^\infty g^{100}(\epsilon)\, d\epsilon = 0, \qquad \int_0^\infty g^{001}(\epsilon)\, d\epsilon = 0,$$

are as defined by Brennan *et al.* and $\partial n/\partial Z$ is the electron density gradient parallel to the electric field $\boldsymbol{E}$, $\partial n/\partial X$ being the gradient perpendicular to both $\boldsymbol{E}$ and $\boldsymbol{B}$. However, as discussed elsewhere (Brennan *et al.* 1990 and GB), for the conditions studied here, the energy distribution function can be adequately represented by dropping the term in $\partial n/\partial X$. Where this expansion is valid, a continuity equation of the form

$$\frac{\partial n}{\partial t} + W_x\frac{\partial n}{\partial X} + W_z\frac{\partial n}{\partial Z} - D_x\frac{\partial^2 n}{\partial X^2} - D_y\frac{\partial^2 n}{\partial Y^2} - D_z\frac{\partial^2 n}{\partial Z^2} - D_{\rm sh}\frac{\partial^2 n}{\partial X\partial Z} = n\nu_{\rm i0} \tag{2}$$

may be used to describe the evolution of the electron number density, $n(\boldsymbol{r},t)$. In the above equation W_x and W_z are components of the swarm drift velocity, while D_x, D_y, D_z are the diagonal components of the diffusion tensor and $D_{\rm sh}$ represent the off-diagonal elements. Further, $\nu_{\rm i0}$ is the swarm averaged ionisation coefficient. Blevin and Brennan (1983) presented an analytic solution for equation (2), which assumed a delta function source of electrons at the cathode and that non-equilibrium effects at the cathode can be neglected. For a steady stream source their solution of equation (2) has the form

$$n(X, Y, Z) = C\exp\left(\frac{W_x X}{2D_x K} + \frac{W_z Z}{2D_z K} - \frac{D_{\mathrm{sh}}(XW_z - ZW_x)}{4D_x D_z K}\right)$$
$$\times\,[ZS_0^{-3/2} K_{3/2}(S_0) + (Z-2d)S_1^{-3/2} K_{3/2}(S_1)],$$

where C is a normalisation constant, while $K = 1 - D_{\mathrm{sh}}^2/4D_x D_z$ and $K_{3/2}$ are modified spherical Bessel functions of the third kind and order 3/2, with arguments

$$S_0^2 = \left(\frac{X^2}{D_x K} + \frac{Y^2}{D_y} + \frac{Z^2}{D_z K} - \frac{D_{\mathrm{sh}} XZ}{D_x D_z K}\right)\left(\frac{W_x^2}{4D_x K} + \frac{W_z^2}{4D_z K} - \frac{D_{\mathrm{sh}} W_x W_z}{4D_x D_z K} - \nu_{\mathrm{i0}}\right),$$

$$S_1^2 = \left(\frac{X^2}{D_x K} + \frac{Y^2}{D_y} + \frac{Z^2}{D_z K} - \frac{D_{\mathrm{sh}} XZ}{D_x D_z K} + \frac{4d(d-Z)}{D_z}\right)$$
$$\times\left(\frac{W_x^2}{4D_x K} + \frac{W_z^2}{4D_z K} - \frac{D_{\mathrm{sh}} W_x W_z}{4D_x D_z K} - \nu_{\mathrm{i0}}\right),$$

where d is the electrode separation. This solution includes single image terms at both the cathode and anode, which constitutes a first order approximation to the effects of an absorbing electrode structure on the discharge.

The justification for the photon flux technique (see e.g. Brennan *et al.* 1990) indicates that the distribution of excited states at a position Z is proportional to the electron number density at a slightly smaller axial position, $Z-\Delta$, where the expansion of equation (1) is valid. Blevin and Brennan (1983) showed that for discharges in $\boldsymbol{E}\times\boldsymbol{B}$ fields, a 'complete' description of the electron number density in terms of the transport parameters can be made by determining the electron concentration integrated along lines of sight in two directions. One is parallel to the magnetic field (Y axis), giving

$$N_y(X, Z) = (C\,Z/S_2)K_1(S_2)\exp\left(\frac{W_x X}{2D_x K} + \frac{W_z Z}{2D_z K} - \frac{D_{\mathrm{sh}}(XW_z + ZW_x)}{4D_x D_z K}\right), \tag{3}$$

where K_1 is a modified Bessel function of the third kind and order 1, with the argument

$$S_2^2 = \left(\frac{X^2}{D_x K} + \frac{Z^2}{D_z K} - \frac{D_{\mathrm{sh}} XZ}{D_x D_z K}\right)\left(\frac{W_x^2}{4D_x K} + \frac{W_z^2}{4D_z K} - \frac{D_{\mathrm{sh}} W_x W_z}{4D_x D_z K} - \nu_{\mathrm{i0}}\right).$$

Similarly, in the direction orthogonal to both fields (X axis), we have

$$N_x(Y, Z) = (C\,Z/S_3)K_1(S_3)\exp\left(\frac{W_z Z}{2D_z K}\right), \tag{4}$$

where

$$S_3^2 = \left(\frac{Y^2}{D_y} + \frac{Z^2}{D_z K}\right)\left(\frac{W_z^2}{4D_z K} - \nu_{\mathrm{i0}}\right).$$

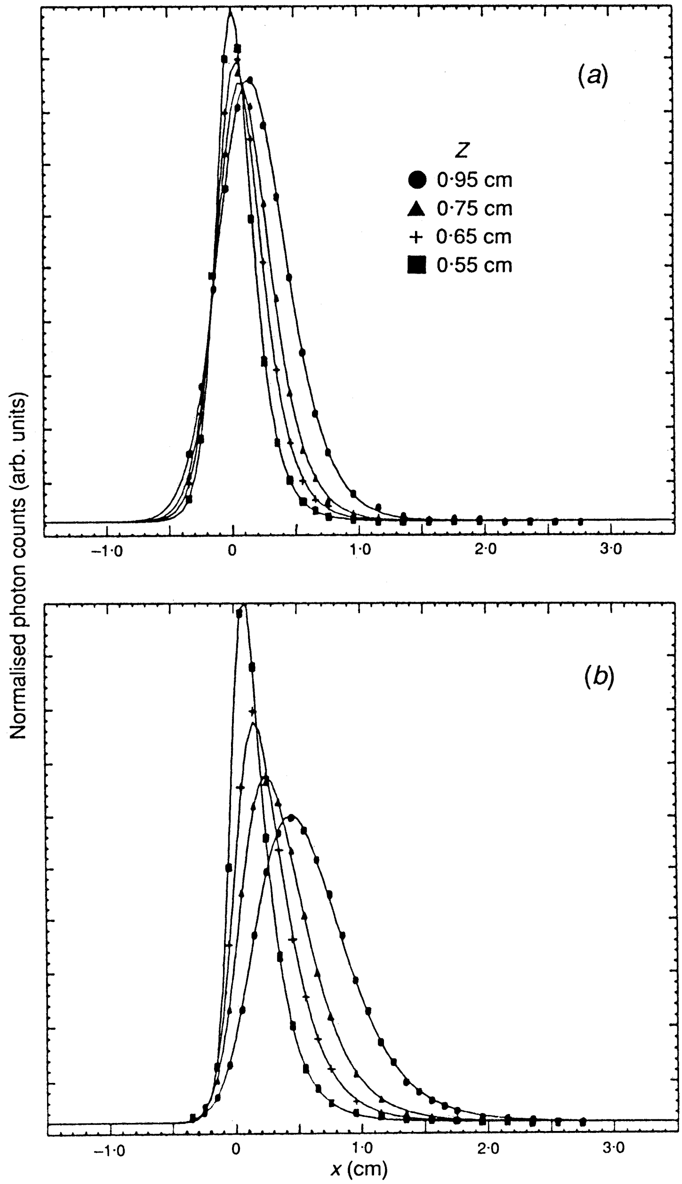

Fig. 2. (*a*) Transverse scan data for $E/N = 350$ Td, $B/N = 283\times10^{-17}$ G cm^3 for the view parallel to the magnetic field. The theoretical curves, at each Z value, use the parameters resulting from a χ^2 fit. (*b*) Similar to that in (*a*), but for $E/N = 465$ Td and $B/N = 1009\times10^{-17}$ G cm^3. Note the good fit to the peaks of the profiles and the effect of the increased magnetic field.

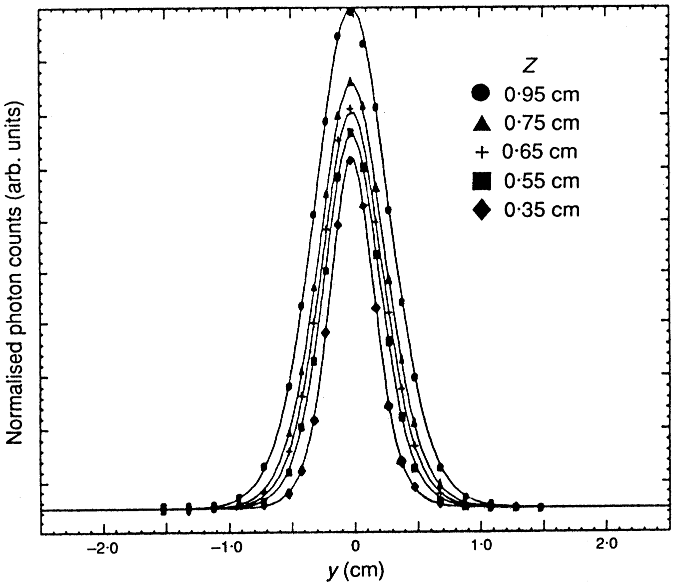

Fig. 3. Transverse scan data and theory for the view orthogonal to the magnetic field at $E/N = 550$ Td and $B/N = 0$. Note that this view is symmetric even for $B > 0$.

Note that the image terms arising due to the presence of the anode at $Z = d$ have been neglected here. This simplifying approximation is valid for measurements at Z positions sufficiently far removed from the anode (this condition was always satisfied in our measurements). Provided that self-absorption of radiation from the discharge can be neglected, along with the motion of an excited molecule in the lifetime of a detected state (~36 ns for the $C^3\Pi_u$–$B^3\Pi_g$ transition at the pressures studied), the relationship between the detected photons and the parent electron distribution is known. Hence, the parameters of (2) were determined by least squares fitting to measurements of the transverse profiles of the photon flux, from the two views, at typically four axial Z positions. Figs 2 and 3 compare typical data for different Z positions (symbols) and 'fitted' theory (solid curves).

The fact that there exists a region of initial non-equilibrium at the cathode, and that the initial electron distribution is not a delta function, may be accounted for by allowing the discharge to have an initial width (see Blevin *et al.* 1976). Equations (3) and (4) may be suitably modified to accommodate this initial width and re-arranged to reveal the 'fitted' parameters W_x/W_z, D_x/μ, D_y/μ, D_z/μ and ν_{i0}/W_z, where μ is the electron mobility in the Z direction, which are independent of the gas density.

Note that the parameter D_{sh} appearing in (3) and (4) is not mentioned above as a 'fitted' parameter; prior to fitting the theoretical expressions to the experimental data, a computational test of the relative sensitivity of (3) and (4) to each of the transport parameters was conducted. This test showed conclusively that, over the range of experimental parameters studied in this work, steady stream experiments are insensitive to the value of D_{sh}. Therefore, the parameter D_{sh} has been omitted from the fitted equations, although it is expected (Brennan *et al.* 1990) to influence a more sensitive time of flight experiment. In an additional test, it was observed that the parameters D_x/μ, D_y/μ and D_z/μ are not completely orthogonal parameters in the context of χ^2 fitting (see below). However, these parameters were used, primarily in order to maintain a conceptual similarity with the earlier work of Wedding *et al.* (1985). The implications of the interdependence of these parameters is discussed further in the next section.

4. Experimental Results

A χ^2 fitting technique was used for determining the transport parameters from the experimental measured photon flux profiles. The use of least squares analysis for fitting multi-parameter theoretical expressions to experimental data is well documented, see e.g. Arndt and McGregor (1966). However, a valid estimation of the uncertainty in the values of the parameters in a multi-parameter space, such as those studied here, may depend in part on the numerical methods used to determine the so called 'χ^2 minimum'. For example, the uncertainties derived from the 'Chifit' program of Bevington (1969) depend on the path taken in the parameter space to the minimum value of χ^2. It was found in the course of this work that Bevington's method failed to produce reliable estimates of the uncertainties in the fitted parameters. The uncertainties quoted in the present results (appearing as error bars in Figs 4 to 6) are derived by finding the maximum and minimum values in each fitted parameter that lead to an increase in the minimum value of χ^2 by one, after allowing the other parameters to vary to locate a new minimum in the reduced space (see Arndt and McGregor). The data and errors were averaged, where data from two or more runs, or 'views', were available.

As mentioned in the Introduction, the experimental results presented in this work are compared with those derived from Monte Carlo calculations detailed in Brennan *et al.* (1990), using the nitrogen gas model proposed by Ohmori *et al.* (1988). Previous computational studies of electron transport in $\boldsymbol{E}\times\boldsymbol{B}$ fields in nitrogen have been conducted by Govinda Raju and Gurumurthy (1978) (Boltzmann equation solution) and recently by Govinda Raju and Dincer (1989) (Monte Carlo). Their transport parameters are based on a highly stylised model of nitrogen, which was constructed without detailed consideration of experimental transport data, to investigate the validity of the so-called 'equivalent field' approach. The arbitrary nature of these cross sections suggests that any agreement with the present results would be largely fortuitous. However, as mentioned, the model proposed by Ohmori *et al.* was optimised for agreement with data from photon flux experiments in electric fields and thus a comparison with the results of this model tests the efficacy of the $\boldsymbol{E}\times\boldsymbol{B}$ configuration in testing cross-section models. Recently, however, the two-term Boltzmann code used by Ohmori *et al.* has been shown to under-estimate the ionisation coefficient α_T (Tagashira and Ohmori, Kelly, personal communications 1990). This is discussed below in relation to the fitted parameter α_T/p_0.

Ratio of the Components of the Drift Velocity

The ratio of the components of the drift velocity, W_x/W_z, is typically determined to within 3% by the fitting procedure. This is illustrated in

Fig. 2 where experimental data, for the view parallel to the magnetic field, is compared with the 'fitted theory' for two experimental conditions at a number of positions along the electric field axis. It can been seen that the fits to the data characterise the changes in the peak positions of the scans, due to the drift in the $\boldsymbol{E}\times\boldsymbol{B}$ direction, very well. The experimental data are compared with the values derived from the Monte Carlo simulations in Fig. 4. On the whole, one can conclude that the cross-section set of Ohmori *et al.* predicts the ratio W_x/W_z very well (curves A–D). The agreement becomes poorer at the highest value of the magnetic field investigated. A comparison using the older cross-section set of Tagashira *et al.* (1980) (curve E) shows the improvement in the newer model over the old.

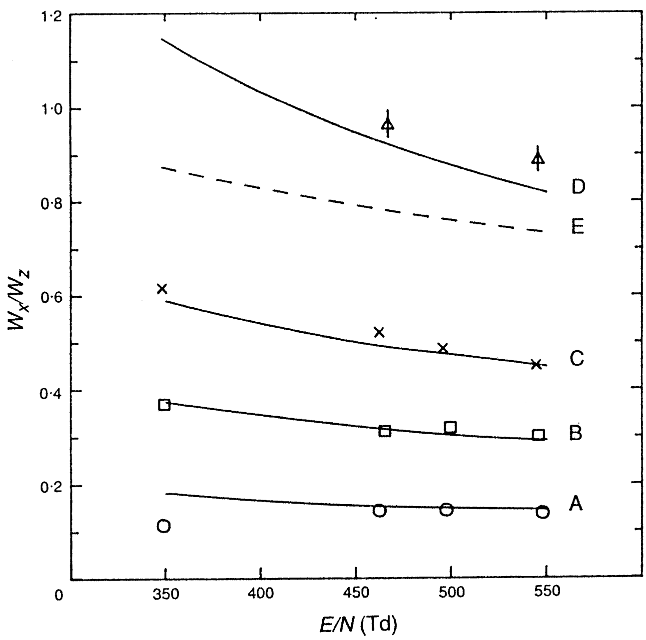

Fig. 4. Comparison of the ratio W_x/W_z between simulations using the nitrogen model by Ohmori *et al.* (1988) and experiment for several similar experimental conditions: curve A, $B/N = 201\times10^{-17}$ G cm^3; curve B, $B/N = 404\times10^{-17}$ G cm^3; curve C, $B/N = 607\times10^{-17}$ G cm^3; and curve D, $B/N = 1009\times10^{-17}$ G cm^3. Note the considerably improved performance of the cross-section set over curve E from Tagashira *et al.* (1980) (see text) at $B/N = 1009\times10^{-17}$ G cm^3. The measurement uncertainty is of the order of the symbol size, except where indicated (see text).

Townsend's First Ionisation Coefficient

Townsend's first ionisation coefficient α_T is not directly measured in these experiments, but must be derived from the expression

$$\alpha_T = \frac{W_z}{2D_z} - \left[\left(\frac{W_z}{2D_z}\right)^2 - \frac{\nu_{i0}}{D_z}\right]^{\frac{1}{2}}.$$

This may be conveniently expanded around ν_{i0}/W_z, giving the first order approximation

$$\alpha_T = \frac{\nu_{i0}}{W_z}\left(1 + \frac{\nu_{i0}}{W_z}\frac{D_z}{\mu}\frac{V}{d}\right),$$

expressed in terms of the fitted parameters ν_{i0}/W_z, D_z/μ and the electric field, V/d, an experimental variable.

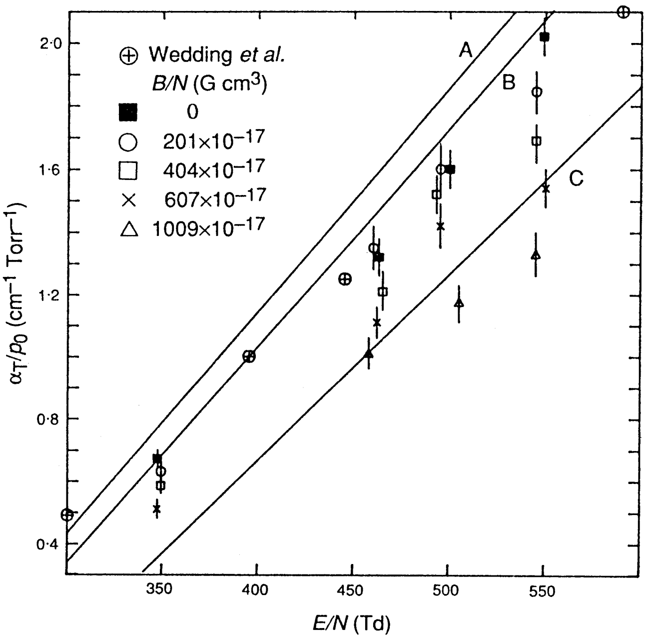

Fig. 5. The ionisation coefficient α_T/p_0. Three simulations are shown: A, for $B/N = 0$; B, for $B/N = 404\times10^{-17}$ G cm^3; and C, for $B/N = 1009\times10^{-17}$ G cm^3. Note that the agreement between simulation A and experiment is poor.

In Fig. 5 the ionisation coefficient, normalised to pressure at 0°C, is plotted against a range of experimental conditions. Here p_0 has been chosen as the normalisation factor, rather than the gas density N, so that a direct comparison with the results of Wedding *et al.* (1985) can be made for the $B = 0$ case. The uncertainty quoted for α_T/p_0 in the present work reflects, in part, the relatively large number of fitted parameters and difficulties experienced in obtaining a good fit to D_z/μ, due to the orthogonality problems alluded to above. In comparison with previous determinations of α_T (see Wedding *et al.*), the better than 7% agreement between the present results for $B = 0$ and those of Wedding *et al.* is satisfactory, given the limited sensitivity of this apparatus in comparison with their time-of-flight techniques. One should note, however, that the present level of agreement with the Wedding *et al.* data for $B = 0$ is roughly twice the uncertainty indicated by the χ^2 fit. Despite this, the agreement for $B = 0$ supports the validity of the present results for nonzero magnetic fields, where the $\boldsymbol{E}\times\boldsymbol{B}$ drift takes the discharge towards the centre of the electrodes, where both the magnetic and electric fields are still more uniform. In the light of the agreement between the simulations of W_x/W_z and our experimental determinations, however, it is disturbing to note the rather larger disagreement between simulation and experiment shown in Fig. 5. Other Monte Carlo simulations for $B = 0$ (Kelly, Tagashira and Ohmori, personal communications 1990) confirm that our calculations of α_T/p_0 for $B = 0$ (curve A) using Ohmori's set are correct, and that Ohmori's Boltzmann code predicts values that are more than 10% lower at these E/N and that the agreement is poorer still at lower E/N. This is a confusing finding since Ohmori *et al.* used the α_T/p_0 data of Wedding *et al.* as a critical test for the cross sections in their model. It can be concluded by comparison with the simulated values (curves B and C, Fig. 5) that, while the nitrogen model predicts the general dependence of α_T/p_0 on E/N and B/N, the model results show a significant departure from experiment at the more extreme conditions.

Components of the Diffusion Tensor

The experiments conducted by viewing photons from an angle orthogonal to both the electric and magnetic fields (Fig. 3) yield a measure of the diffusion parallel to the magnetic field D_y. The data taken from this view have a qualitative similarity to the steady stream experiments of Wedding *et al.* in that there is a symmetry axis about $Y = 0$. Note that no simple quantitative comparison can be made, as the energy distribution function is weighted by the presence of a magnetic field in the integrals defining the diffusion coefficient (see Brennan *et al.*). Analysis of the data taken from this view, using equation (4), yields the pressure independent coefficient D_y/μ. These results are presented in Fig. 6*a*. The process of fitting the theoretical equations to the transverse scan data does not yield an extremely precise measurement of the changes in width, due to diffusion, in the steady stream configuration. However, these results represent the first of their type under these experimental conditions.

Due to the uncertainties in the present values and indeed the failure of the model to predict α_T/p_0 for $B = 0$, it is difficult to draw conclusions from a comparison between the present data and simulated values for D_y/μ. However, the results of the simulations for $B/N = 0$ and 1009×10^{-17} G cm^3 (curves A and B) are plotted in Fig. 6*a* for completeness. Simulated results for D_y/μ for magnetic fields between these two extremes lie between curves A and B. In addition, while not shown in Fig. 6*a*, the present results for zero magnetic field agree with those of Wedding *et al.* within experimental error.

Returning to Fig. 3, it is not surprising that the analysis of data from this 'view' is relatively insensitive to the value of D_z/μ, which is related to the diffusion parallel to the electric field. The sensitivity of D_z/μ is improved by viewing the discharge parallel to the magnetic field and the uncertainty decreases with increasing magnetic field strength. This is reflected in the values of Fig. 6*b*, which are plotted along with the predictions of the simulation for the minimum (curve A) and maximum (curve B) magnetic field strength studied. The increased accuracy in D_z/μ is achieved at the expense of the sensitivity in D_x/μ, as indicated in Fig. 6*c*. Note that simulated values of D_x/μ rise almost immediately from $B = 0$ to a maximum near $B/N = 404\times10^{-17}$ G cm^3 (curve A) over the range of E/N studied, then decrease rapidly with increasing

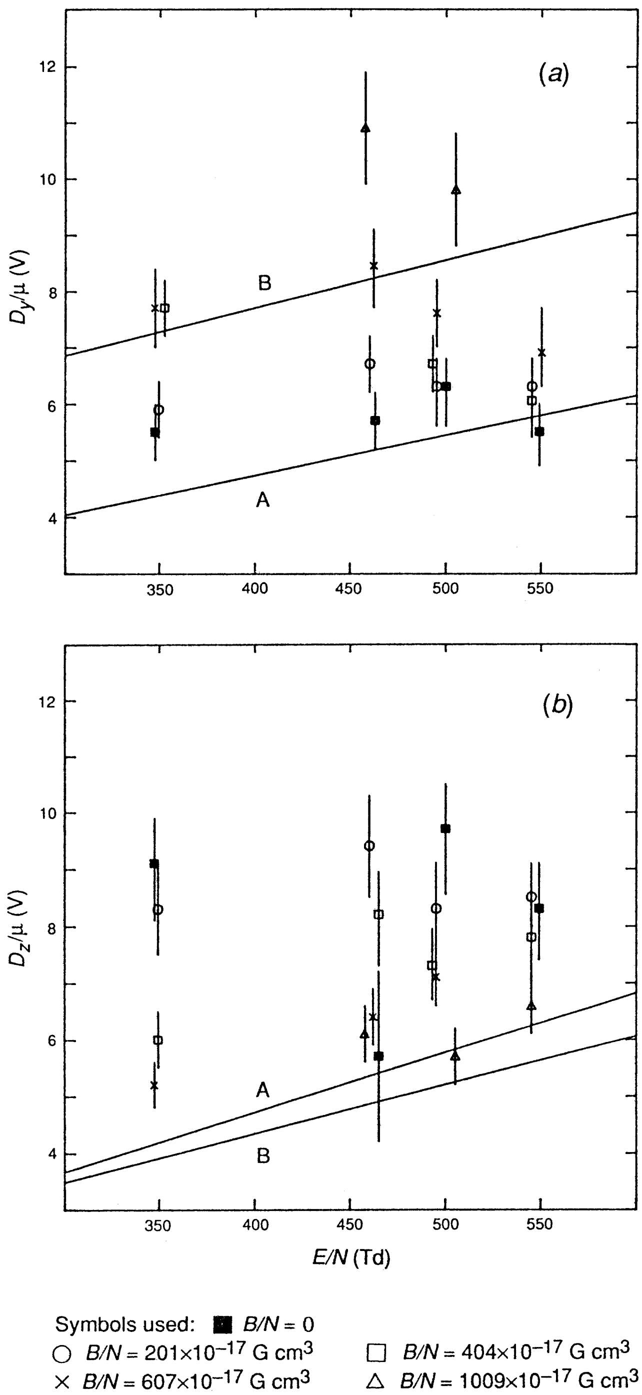

Fig. 6. The ratios (*a*) D_y/μ, (*b*) D_z/μ and (*c*) D_x/μ. In each case simulation B is for $B/N = 1009\times10^{-17}$ G cm^3. Simulation A is for $B/N = 0$ in parts (*a*) and (*b*) and for $B/N = 404\times10^{-17}$ G cm^3 in part (*c*).

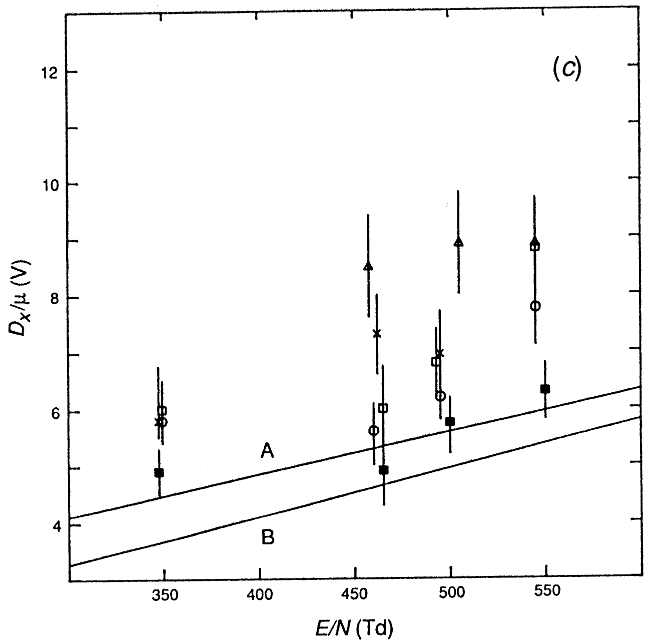

Fig. 6c

magnetic field strength (curve B). As discussed by Brennan *et al.*, the diffusion across the magnetic field lines decreases with increasing field strength, but the electron mobility μ decreases more rapidly for small magnetic fields; hence the initial increase in the ratio D_x/μ.

5. Conclusions

The measurements described above represent the first results in nitrogen under these conditions. Despite the relatively large uncertainty in some of the parameters that this type of experiment yields, there is clearly some discrepancy between the parameters derived from the simulations and the experiments. Although the agreement for W_x/W_z using the model of Ohmori *et al.* shows considerable improvement over that of Tagashira *et al.*, there is a significant level of disagreement for the parameter α_T/p_0. The good agreement (better that 4% for a α_T between 200 and 500 Td, $B = 0$) between the Monte Carlo simulations conducted in the course of this work and those performed by Kelly and by Tagashira and Ohmori suggests an error in the two-term code used by Ohmori *et al.* However, the precise nature of this error is unknown and warrants further investigation and possible modification to the cross-section set. It should be emphasised that a primary objective of the investigation was to test whether the information from $\boldsymbol{E}\times\boldsymbol{B}$ experiments could be used to further test the 'validity' of gas models that describe discharge behaviour in electric fields in addition to measuring the fundamental transport parameters. Unfortunately, such a test does not give any indication of which cross sections are in error, or whether any need to be included in the model. A more accurate determination of the transport parameters, especially the elements of the diffusion tensor, clearly awaits the more sophisticated time of flight experiments.

Acknowledgments

This work was funded by the Australian Research Grants Scheme and the Flinders University Research Committee. The authors thank H. A. Blevin and L. J. Kelly for their support in various aspects of this work.

References

Arndt, R. A., and McGregor, M. H. (1966). *Meth. Comp. Phys.* **6**, 253.
Bevington, P. R. (1969). 'Data Reduction and Error Analysis for the Physical Sciences' (McGraw–Hill: New York).
Blevin, H. A. (1985). XVII Int. Conf. on Phenomena in Ionised Gases, Invited papers, Budapest (Eds J. S. Bakos and Z. S. Uzsa Sörlia), p. 308.
Blevin, H. A., and Brennan, M. J. (1983). *Aust. J. Phys.* **36**, 859.
Blevin, H. A., Fletcher, J., and Hunter, S. R. (1976). *J. Phys.* D **9**, 1671.
Brennan, M. J., Garvie, A. M., and Kelly, L. J. (1990). *Aust. J. Phys.* **43**, 27.
Crompton, R. W. (1983). XVI Int. Conf. on Phenomena in Ionised Gases, Invited papers, Dusseldorf (Eds W. Botticher *et al.*), p. 58.
Garvie, A. M., and Brennan, M. J. (1990). *Aust. J. Phys.* **43**, 779.
Govinda Raju, G. R., and Dincer, M. S. (1989). Poster session, Sixth Int. Swarm Seminar, New York (Eds E. E. Kunhardt and R. J. Van Brunt).
Govinda Raju, G. R., and Gurumurthy, G. R. (1978). *Int. J. Electron.* **44**, 355.
Jelenkovic, B. M., and Phelps, A. V. (1987). *Phys. Rev.* A **36**, 5310.
Ohmori, Y., Shimozuma, M., and Tagashira, H. (1988). *J. Phys.* D **21**, 724.
Phelps, A. V., and Pitchford, L. C. (1985). *Phys. Rev.* **31**, 2932.
Tachibana, A., and Phelps, A. V. (1979). *J. Chem. Phys.* **71**, 3544.
Tagashira, H., Taniguchi, T., and Sakai, Y. (1980). *J. Phys.* D **13**, 235.
Wedding, A. B., Blevin, H. A., and Fletcher, J. (1985). *J. Phys.* D **18**, 2351.

Manuscript received 4 June, accepted 25 September 1990